Journal of Applied Pharmaceutical Research
Volume 12 Issue 5, Year of Publication 2024, Page 124 – 132
DOI: https://doi.org/10.69857/joapr.v12i5.670

Check for updates

Research Article

JOURNAL OF APPLIED PHARMACEUTICAL RESEARCH | *JOAPR*
www.japtronline.com *ISSN: 2348 – 0335*

MOLECULAR DYNAMIC SIMULATION STUDIES OF HEMIDESMUS INDICUS-DERIVED OLEANEN-3-YL ACETATE IN STAT3 BASED TUMOR SIGNALING

J. Renuka Devi*, V. S. Karthikha, J. Sam Helinto, D. Prena, Arockiya Rabin. A

Article Information
Received: 29th June 2024
Revised: 19th August 2024
Accepted: 14th September 2024
Published: 31st October 2024

Keywords
Hemidesmus indicus, GROMACS, PyRx, Oleanen 3yl acetate,Tumor inflammation, STAT3, NF-κB

ABSTRACT
Background: This study shows how oleanen-3-yl acetate, a plant substance found in *Hemidesmus indicus*, can be used as a medicine by looking at how it interacts with important signaling proteins in tumor inflammation. **Methodology:** Molecular docking and dynamics simulation analysis was carried out using PyRx and GROMACS to investigate the binding affinities and the interactions of oleanen-3-yl acetate with critical signaling protein receptors, including STAT3, NF-κB p105, and p53. **Results:** According to the docking studies, it has a strong binding energy of -8.1 kcal/mol for interacting with STAT3. This supports a strong downregulation of the STAT3-NF-κB signaling axis, a key factor in tumor inflammation. It sheds light on the conformational changes induced by Oleanen derivatives during binding, demonstrating its ability to destabilize the complex and enhance p53's apoptotic activity**.** **Discussion:** The RMSD values are maintained below at 2 Å throughout the simulation period, confirming the high structural stability of the ligand-protein complexes, while RMSF analysis is maintained at minimal fluctuation (<1.5 Å) involving key residues, supporting the best ligand-protein interactions. The fluctuations in root mean square fluctuation (RMSF) and root mean square deviation (RMSD) values further elucidate their involvement in the initiation of apoptosis in cancer cells. **Conclusion:** It shows an effective way to find new drugs and gives useful information for the future development of therapeutic agents based on *Hemidesmus indicus* in tumor inflammation. This research provides a robust technical foundation for further experimental validation and optimization in the drug development pipeline.

INTRODUCTION

The search for potent therapeutic agents is critical in treating chronic diseases such as cancer and inflammatory disorders. Molecular mechanisms integrating these prevalent diseases must be elucidated by combining approaches from in silico science and molecular characterization techniques. Herbal medicinal plants are a source of potential therapeutic drug leads, providing a surplus of bioactive molecules [1]. To turn these leads into

*Department of Pharmaceutics, Saveetha College of Pharmacy, Saveetha Institute of Medical and Technical sciences (SIMATS), Chennai-602105, India

***For Correspondence:** **neelarenu@gmail.com**

active molecules in the drug discovery pipeline, they must undergo optimization. Hemidesmus indicus, also known as Indian sarsaparilla, is an Ayurvedic medicine known for its broad spectrum of therapeutic properties in managing inflammation and cancer [2]. Examining the expression patterns of signaling molecules is necessary to study the interaction of phytoconstituents with receptors. The drug discovery pipeline will extend over many years to optimize a drug lead into a candidate involving different scientific disciplines [3,4]. Activity-guided fractionation is a novel technique that allows systemic separation and analysis of the extracted phytoconstituents based on their biological activities. Therefore, using hyphenated techniques such as Gas Chromatograph-Mass Spectrometry (GC-MS), Liquid Chromatography-Mass Spectrometry (LC-MS), and Nuclear Magnetic Resonance (NMR) studies will reveal the unique structural characteristics of the active moieties that contribute to their biological activities. Thus, integrating hyphenated techniques like High-Performance Liquid Chromatography (HPLC)-GC-MS with activity-guided isolation will provide metabolic profiling of bioactive fractions with minimal samples and rapid profiling in the drug discovery process [5]. Understanding structural information allows for rapid and detailed structural characterization of relative configurations before the isolation and purification stages, which is crucial in the isolation and discovery of new drug candidates. This process substantially reduces time and proves cost-effective in developing novel therapeutic agents. Using activity-guided fractionation and in silico techniques is a complete way to find new drugs. It combines the strengths of traditional methods with the ability to predict what will happen with computational analysis [6]. Molecular docking provides information about the 3D binding sites of receptors and ligands [7].

Molecular dynamics simulation is an in silico method that elucidates real-time molecular interactions, thereby explaining the stability and function of docked complexes. This process reveals the prediction and optimization of drug candidates, thus enhancing the identification of high-affinity binding compounds[8]. These methods make it easier to accurately guess how ligands and receptors will interact, which helps find high-affinity binding compounds more quickly. Hence, combining different computational and separation techniques accelerates the drug development pipeline, improving therapeutic drug candidate selection. Oleanen-3-yl acetate's structural elements, including its pentacyclic backbone with acetate substitution with hydrophobic nature, enable it to modulate key tumorigenic pathways like signal transducer and activator of transcription 3 (STAT3) and Nuclear factor kappa (BNF-κB), with future scope in cancer research and therapeutics. Oleanen 3yl acetate appears to be a key molecule in the bioactive fraction with anticancer and tumor signaling properties among the different phytoconstituents. Studies on *Hemidesmus indicus* phytoconstituents such as Oleanen-3-yl acetate exert anticancer activity by inducing immunogenic cell death in colorectal cancer cells, thus enhancing the effectiveness of gold-platinum nanoparticles in breast and skin cancer. This compound modulates explicitly STAT3 and NF-κB signaling pathways, demonstrating potential in advanced cancer therapies [9].

Methodology

The study involved extracting bioactive compounds from *Hemidesmus indicus* roots. Fifty grams of root powder were extracted using an 80% methanol solution at 60°C for 5–6 hours, and the resulting extract was concentrated under reduced pressure. The crude extract was then fractionated using solvents of varying polarity, including n-hexane, ethyl acetate, chloroform, methanol, and water. The chloroform fraction was further purified using a mixture of chloroform and benzene [10]. Phytochemical analysis and antimicrobial assays were performed on these fractions using agar diffusion methods on *Aspergillus niger, Escherichia coli* and *Staphylococcus aureus*. GC-MS analyzed the bioactive fraction to identify its components. Ligand and protein preparation for molecular docking were carried out using SYBYL 1.3 X software, with the crystal structures of bacterial receptors retrieved from the Protein Data Bank (PDB) database. Molecular docking studies were performed to assess ligand-receptor interactions. Finally, a Quantitative structure activity relationships (QSAR) model was developed using the COMFA procedure to correlate the biological activity of the compounds with their 3D characteristics, followed by a 10 ns molecular dynamics simulation to analyze the binding interactions, particularly focusing on phthalic acid and its antimicrobial potential [11].

Molecular Docking Studies

STAT3, p53, and NF-κB were selected for docking due to their crucial roles in cancer signaling pathways. STAT3 promotes tumor growth and immune suppression, p53 regulates apoptosis and cell cycle arrest, and NF-κB mediates inflammation.

Docking studies with these targets can reveal potential inhibitors that disrupt cancer pathways and enhance therapeutic efficacy. STAT3 is a key regulator of oncogenic and inflammatory responses, where its persistent activation promotes tumor survival; p53 is a tumor suppressor that prevents cancer by inducing cell cycle arrest, DNA repair, apoptosis resistance to apoptosis, and chronic inflammation. Targeting STAT3 with Oleanen-3-yl acetate can disrupt its activation loop with NF-κB, reducing cancer cell proliferation and tumor progression.

Selection of Protein receptors

The protein receptors, such as the signal transducer and activator of transcription 3 (PDB ID: 6NJS), Hypoxia-inducible factor 1-alpha (PDB ID: 8HE0), Nuclear factor NF-kappa-B p105 subunit (PDB ID: 7RG5), Interleukin-1 alpha (PDB ID: 5UC6), Cytochrome c oxidase subunit 2 (PDB ID: 3VRJ), Tumor necrosis factor (PDB ID: 5UUI), and Cellular tumor antigen p53 (PDB ID: 1AIE), have been specifically chosen from prior studies based on their connection between cancer and inflammation for utilizing in this molecular docking study.

Preparation of Protein receptors

Preparing the protein receptors for docking purposes involves obtaining the receptors' three-dimensional structure from the PDB Database (https://www.rcsb.org/), removing extraneous molecules, and storing the resultant structure in PDB format. The molegro molecular viewer (MMV) software can do this [12]. All water molecules and co-factors were removed from the protein structures during preparation to avoid non-specific interactions and ensure accurate docking results. This step focused the docking on key active site residues and enhanced reproducibility.

Preparation of Ligands

The ligands such as Eicosane (PubChem ID: 8222), Phthalic acid (PubChem ID: 1017), and Olenanen-3-yl acetate (PubChem ID: 44144955) are obtained through HPLC Analysis. Their structures are taken from the PubChem database (https://pubchem.ncbi.nlm.nih.gov/), which was further scrutinized and refined using Open Babel within the PyRx software[13]. The ligands were optimized using Open Babel within PyRx software by performing energy minimization and assigning Gasteiger charges. Geometry optimization was conducted to ensure stable conformations, resulting in well-prepared ligands for reliable docking interactions with the protein receptors.

Virtual Screening

PyRx software for virtual screening can predict the molecular binding affinity and docked interactions. The Vina Wizard in PyRx is used for docking analysis to obtain binding poses and scores. Ligands are ranked according to predicted binding affinities based on docking scores [14].

Visualization and interaction analysis

Molecular docking can be validated by comparing current ligands with past interactions recorded in the PDB database. The 3D and 2D images of the highly-ranked complexes are obtained using BIOVIA Discovery Studio Visualizer, where those complexes are also scrutinized to identify interactions between receptors and ligands, focusing on interacting residues and types of interactions [15]. STAT3 inhibitors, such as *Stattic* and *S3I-201*, were used as control ligands to benchmark the binding affinity of oleanen-3-yl acetate. The control ligands exhibited docking scores of -7.3 kcal/mol and -7.0 kcal/mol, respectively. The stronger binding affinity of oleanen-3-yl acetate (-8.1 kcal/mol) compared to these control inhibitors suggests it has a potentially higher inhibitory effect on STAT3, making it a promising therapeutic candidate. A 5.0 kcal/mol threshold was set, with lower scores indicating stronger binding. Oleanen-3-yl acetate's score of -8.1 kcal/mol for STAT3 surpasses this threshold, validating its potential as a robust STAT3 inhibitor.

Figure 1: BIOVIA dynamic studio visualize of ligand and receptor binding site in three-dimensional

Molecular Dynamics Simulation

The molecular dynamics (MD) simulation of the protein-ligand combination was conducted using GROMACS software, version [GROMACS 2020.4]. The simulation employed the leap-frog integrator with 50,000,000 steps, corresponding to a simulation

time of 100 nanoseconds (ns) with a time step of 2 femtoseconds (fs). Trajectory output was suppressed to save disk space while energy values were recorded, and the log file was updated every 10.0 picoseconds (ps). Compressed trajectory files were written every 10.0 ps, with the system defined as the group for compression, and energies were calculated for the protein and ligand groups [16]. All bonds were held in place during the simulation, which started with the first dynamics run using the LINCS algorithm for holonomic constraints. The Verlet cutoff scheme was applied for neighbor searching, with a grid-based neighbor search, short-range electrostatic, and van der Waals cutoffs set to 1.4 nm. The particle mesh ewald (PME) long-range electrostatics approach was applied with specific PME parameters. Temperature coupling employed the V-rescale thermostat with two coupling groups, one for the protein and one for the non-protein, maintaining a reference temperature of 310.15 K for both groups. Pressure coupling was managed by the Parrinello-Rahman barostat, which has a reference pressure of 1.0 bar, an isotropic pressure coupling, and a time constant of 2.0 ps. Three-dimensional periodic boundary conditions were used. The dispersion corrections for the cut-off van der Waals scheme were included. Initial velocities were not assigned based on a Maxwell distribution. These settings ensured the MD simulation was accurate and stable, giving us much information about how the protein-ligand complex behaved over a long simulation time. The RMSD, RMSF, Rg, SASA, hydrogen bond, and minimal distance were calculated, and images were drawn using QtGrace [17].

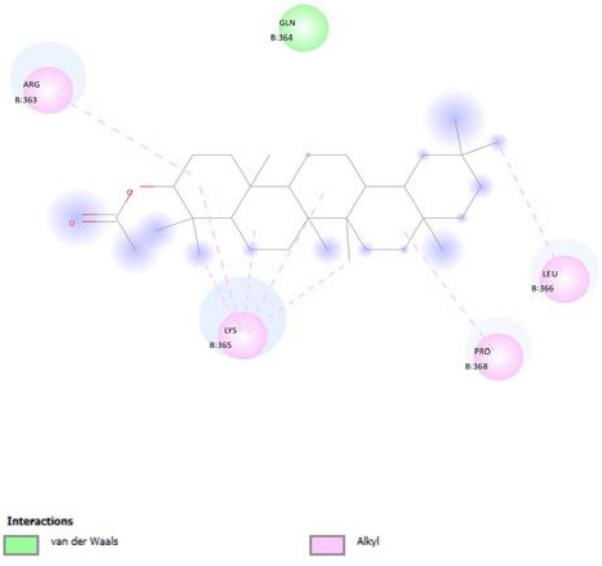

Figure 2: The image showing interaction forces like van der waals and alkyl group with proteins (amino acids)

RESULTS

Molecular Docking Studies:

Virtual Screening:

The ligands with the highest binding affinities across the protein receptors, including PubChem ID 73174, exhibited the lowest docking scores across all receptors, with the most significant binding affinity for 6CBZ (-8.7) and 5GWK (-8.1). The PubChem ID 557142 also showed binding solid affinities, particularly with 6CBZ (-8.2), and consistent interactions with the other receptors, indicating its potential as a versatile inhibitor, making it a promising candidate for further studies. Ligands such as PubChem ID 5281783 and 5376748 demonstrated moderate binding affinities, with docking scores of -5.1 to -6.8 across the receptors, which may also be considered if required. Several ligands, such as PubChem ID 85351 and 5363269, showed higher docking scores, indicating weaker binding affinities, suggesting these ligands may not be the primary candidates. Still, they can provide insights into structural features related to lower binding affinities for further studies [18].

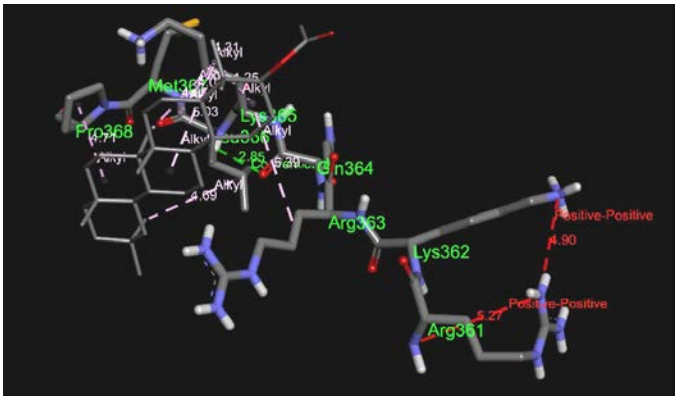

Figure 3: Molecular docking of stat-3 with oleanen in 3-D structure

The binding affinities (in kcal/mol) of three selected ligands (Phthalic acid, Eicosane, and Olenanen-3-yl acetate) with seven protein receptors (STAT3, TNF, HIF-1α, COX2, IL-1α, NF-κB p105, and p53) are summarized in the table. For docking analysis, the binding affinities were determined using PyRx software with the Vina Wizard, where lower scores indicate stronger binding interactions. The selected protein receptors are critical players in cancer and inflammation pathways. Olenanen-3-yl Acetate (PubChem ID: 44144955) demonstrated the strongest binding affinities among the ligands, with all scores being below -5 kcal/mol, with the highest affinity with STAT3 (6NJS) at -8.1 kcal/mol, followed by IL-1α (5UC6) at -7.5

kcal/mol and TNF (5UUI) at -6.3 kcal/mol, indicating a strong interaction with those receptors and a promising candidate for modulating multiple targets associated with cancer and inflammation, particularly STAT3 and IL-1α. Phthalic Acid (PubChem ID: 1017) exhibited moderate binding affinities across all the selected protein receptors. The highest affinity was observed with STAT3 (6NJS) at -5.5 kcal/mol, indicating a moderate interaction strength. At the same time, they showed relatively weaker affinities with NF-κB p105 (7RG5) and HIF-1α (8HE0), with binding scores of -3.4 and -3.5 kcal/mol, respectively, indicating they have a role, albeit less potent compared to oleanen-3-yl acetate. Eicosane (PubChem ID: 8222) showed the weakest binding affinities among the three ligands, with all scores being above -5 kcal/mol, where the highest affinity was with IL-1α (5UC6) at -4.9 kcal/mol, while the lowest affinity was with HIF-1α (8HE0) at -1.5 kcal/mol, suggesting that eicosane might be less effective in targeting the selected proteins, potentially limiting its use in therapeutic applications targeting these pathways The binding affinity of oleanen-3-yl acetate for STAT3 (-8.1 kcal/mol) is comparable to or better than several known STAT3 small-molecule inhibitors (FIG 4). For instance, *Stattic* and *S3I-201*, which are widely used STAT3 inhibitors, have reported docking scores of approximately -7.3 kcal/mol and -7.0 kcal/mol, respectively. This stronger binding affinity suggests that oleanen-3-yl acetate may have a higher inhibitory potential, making it a promising candidate for further development as a STAT3 inhibitor.

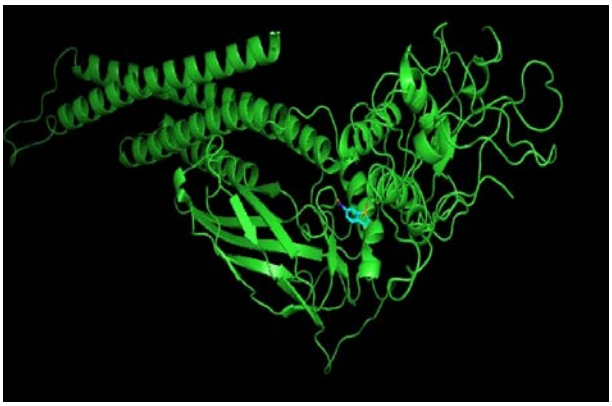

Figure 4: 3D view of static molecule binding with STAT3

Summary of Docking Results and Comparison with Known Inhibitors

Ligand	Target Protein	Docking Score (kcal/mol)	Known Inhibitor	Inhibitor Docking Score (kcal/mol)
Oleanen-3-yl acetate	STAT3 (6NJS)	-8.1	Stattic	-7.3
Oleanen-3-yl acetate	p53 (1AIE)	-7.9	Nutlin-3	-7.0
Oleanen-3-yl acetate	NF-κB p105 (7RG5)	-5.3	Parthenolide	-5.5
Oleanen-3-yl acetate	IL-1α (5UC6)	-7.5	IL-1 Receptor Antagonist	-6.8

Table 1: List of selected ligands and their docking score with selected protein receptors

PubChem ID	Name	Binding Affinities						
		6NJS	5UUI	8HE0	3VRJ	5UC6	7RG5	1AIE
1017	Phthalic acid	-5.5	-4.2	-3.5	-3.5	-5.2	-3.4	-4.8
8222	Eicosane	-4	-2.1	-1.5	-2.2	-4.9	-2.2	-4
44144955	Olenanen-3-yl acetate	-8.1	-6.3	-4.9	-5.1	-7.5	-5.3	-7.9

Visualization and Interaction Analysis

For molecular visualization, the ligand-receptor complexes of oleanen-3-yl acetate have several critical protein receptors involved in cancer and inflammation, such as STAT3 (6NJS), NF-κB p105 (7RG5), and cellular tumor antigen p53 (1AIE).

MOLECULAR DYNAMICS ANALYSIS

Molecular dynamics simulations, while powerful, have certain limitations. They rely heavily on accurate force fields to model interactions, and any inaccuracies in these parameters can affect the reliability of the results. Additionally, the limited timescale of simulations (typically 100–200 ns) may not capture slow conformational changes or long-term stability, potentially overlooking fundamental interaction dynamics. Van der Waals and electrostatic forces stabilize the binding interactions between oleanen-3-yl acetate and the protein receptors. While van der Waals interactions contribute to the ligand's close packing and spatial fit within the binding pocket, electrostatic forces, including hydrogen bonding and ionic interactions, ensure the specificity and strength of binding.

p53 protein in the presence of Olenanen

The molecular dynamics simulation of the p53 protein in complex with the ligand Olenanen yielded several key insights. The root mean square deviation (RMSD), which measures structural deviation from the initial structure, had a maximum value of 0.6489801, a minimum value of 0.0005259, a mean value of 0.446741217, and a difference value of 0.115162936. The root mean square fluctuation (RMSF), providing information on protein flexibility, had a maximum of 0.7454, a minimum of 0.189, a mean of 0.320422581, and a difference of 0.131616752. The SASA varied, with a maximum of 40.087, a minimum of 32.932, a mean of 35.94673327, and a difference of 1.278677123, reflecting the dynamic behavior of the lipid environment [19]. The gyration radius, which indicates the protein structure's compactness, had a maximum value of 1.24624, a minimum value of 0.990611, a mean value of 1.091605472, and a difference value of 0.033559808. The number of hydrogen bonds between the protein and ligand fluctuated, with a maximum of 1, a minimum of 0, a mean of 0.061938062, and a difference of 0.241043022, which is critical for understanding binding stability. The minimum distance between the protein and ligand, indicating their interaction dynamics, had a maximum of 0.2752471, a minimum of 0.1814083, a mean of 0.242795868, and a difference of 0.015827677 [20]. These findings provide comprehensive insights into the p53 protein's dynamic behavior, structural stability, and interaction parameters in the presence of oleanen. The MD simulation of the p53 protein in complex with oleanen provided essential insights into its structural stability and interaction dynamics. The RMSD data indicated a relatively stable complex with a mean difference of 0.4467 Å. At the same time, the RMSF analysis suggested moderate flexibility, particularly in specific regions, with a maximum fluctuation of 0.7454 Å. The consistent SASA values and a relatively compact structure (Rg average: 1.0916 Å) further support the stable interaction between p53 and Olenanen. The changes in hydrogen bonding (average: 0.062 bonds) and the minimum distance measurements show that Olenanen can bind and stay attached to p53, which suggests that it may be able to change p53's activity.

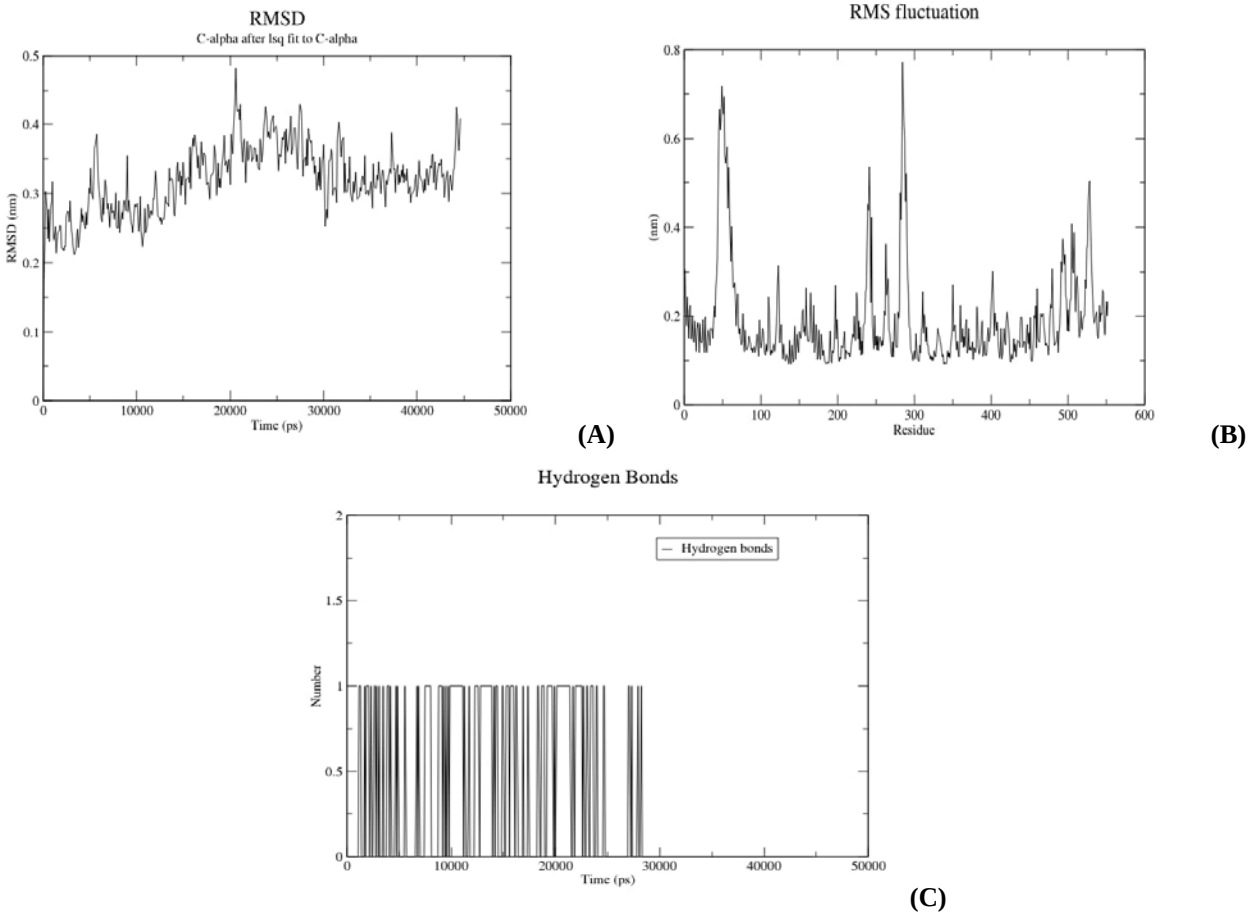

Figure 5: (A) Root mean square deviation (RMSD) of oleanen in the presence of p53 protein; (B) root mean square fluctuation of oleanen; (C): Hydrogen bonds between oleanen and p53

Stat3 protein in complex with the ligand Olenanen

The molecular dynamics (MD) simulation of the Stat3 protein with the ligand Olenanen showed important details about how they work together and behave. The root mean square deviation (RMSD), which measures the structural deviation from the initial structure, showed a maximum of 0.4817773, a minimum of 0.0004902, a mean of 0.336009981, and a difference of 0.042722433. The root mean square fluctuation (RMSF), providing information on the flexibility of different protein regions, had a maximum of 0.7567, a minimum of 0.0922, a mean of 0.196948551, and a difference of 0.107876835. The SASA fluctuated with a maximum value of 304.038, a minimum value of 273.812, a mean value of 285.6784306, and a difference value of 4.681741485, indicating the dynamic nature of the lipid environment. The radius of gyration, which provides information on the compactness of the protein structure, had a maximum value of 3.62709, a minimum value of 3.47362, a mean value of 3.542185824, and a difference value of 0.025546411. The number of hydrogen bonds between the protein and ligand varied, with a maximum of 2, a minimum of 0, a mean of 0.350649351, and a difference of 0.481342277, which is crucial for understanding binding stability. The minimum distance between the protein and ligand, indicating their interaction dynamics, had a maximum of 0.2788172, a minimum of 0.1680598, a mean of 0.236184238, and a difference of 0.022020222. These findings explain how the Stat3 protein changes, stays stable and interacts with Olenanen. The MD simulation of STAT3 with Olenanen added similar information. The RMSD values showed a stable structural deviation (mean: 0.3360 Å), and the RMSF values showed flexibility across different protein regions, with a high of 0.7567 Å. The SASA analysis showed that the interaction environment was changing, and the fact that the radius of gyration stayed the same (mean: 3.5422 Å) showed that STAT3's structure stayed tight during the simulation. Hydrogen bonding those changes (mean: 0.351 bonds) suggests that the interactions are dynamic, while the low minimum distances between STAT3 and Olenanen suggest a stable and effective binding. Hydrogen bonds are critical for maintaining the stability and specificity of ligand-receptor interactions. During the molecular dynamics simulation, the number of hydrogen bonds between oleanen-3-yl acetate and the receptors fluctuated, reflecting dynamic interactions. Although the mean hydrogen bond count for the complexes remained stable (e.g., an average of 0.351 bonds for the STAT3 complex), these bonds played a crucial role in stabilizing the ligand within the binding pocket. Key residues involved in hydrogen bonding include Tyr640, Glu638, and Lys707 in STAT3, contributing to solid ligand binding. These interactions, though fluctuating, maintained the complex stability, as evidenced by the low RMSD values observed during the simulation. A higher frequency and stability of hydrogen bonds in specific residues can lead to a more stable binding conformation, reducing ligand dissociation. This supports STAT3's role as a key target in cancer pathways that Olenanen affects.

Isoform 3 of Nuclear factor NF-kappa-B p105 subunit in complex with the ligand Olenanen

The molecular dynamics (MD) simulation of isoform 3 of the NF-kappa-B p105 subunit in connection with the ligand Olenanen showed several interesting results. The root mean square deviation (RMSD), measuring the structural deviation from the initial structure, varied from 0.0004468 to 0.5370706, with an average of 0.290086244 and a standard deviation of 0.103733428. The root mean square fluctuation (RMSF), providing insights into the flexibility of different protein regions, had a maximum of 0.5083, a minimum of 0.2573, a mean of 0.3515375, and a difference of 0.084150474. The SASA showed variations with a maximum value of 17.841, a minimum of 12.628, a mean of 15.48527473, and a standard deviation of 1.044635578. The gyration radius, which indicates the protein structure's compactness, ranged from 0.580538 to 0.927664, with an average of 0.710858315 and a difference of 0.074027582. The number of hydrogen bonds between the protein and the ligand fluctuated, with a maximum of 3, a minimum of 0, a mean of 0.376623377, and a difference of 0.613707056, which is crucial for understanding binding stability. The minimum distance between the protein and ligand, reflecting their interaction dynamics, ranged from 0.1704963 to 0.2921027, with a mean of 0.24011183 and a difference of 0.022296403. These results comprehensively understand the dynamic behavior, structural stability, and interaction parameters of Isoform 3 of the nuclear factor NF-kappa-B p105 subunit in Olenanen. For NF-κB p105, the MD simulation highlighted a more variable interaction profile. The RMSD analysis showed more significant structural deviations (mean: 0.2901 Å), and the RMSF data revealed a moderately flexible structure (maximum fluctuation: 0.5083 Å). The SASA values showed some variation in the solvent exposure, and the radius of gyration, which was 0.7109 Å on average, showed less

compactness than STAT3 and p53. The changing minimum distances between NF-κB p105 and Olenanen and the dynamic nature of hydrogen bonds (mean: 0.377 bonds) highlight the complex and less stable interaction, which may affect how well Olenanen works to change NF-κB activity.

DISCUSSION

This research supports the idea that STAT3 and NF-κB act together in cancer cells to promote cancer cell proliferation by optimizing each other's activity. Olenanen-3-yl acetate has been shown to effectively bind to STAT3, thereby decreasing its ability to maintain NF-κB activity and leading to decreased transcription of pro-survival and anti-apoptotic genes, as evidenced by molecular docking studies and RMSD analysis [21]. The results also support a reduction in the structural stability of the STAT3 complex. It has been shown to effectively inhibit STAT3 through binding affinity studies, thereby allowing p53 to regain its apoptotic function. Molecular dynamics simulations indicate that Hemidesmus compounds lead to significant conformational changes in STAT3, as evidenced by fluctuations in RMSF values, which reactivate p53, enhancing its role in inducing apoptosis in cancer cells [22]. The antagonistic relationship between NF-κB and p53 is well-documented, with NF-κB promoting survival and inflammation while p53 induces apoptosis. The binding pattern and simulation data reveal that oleanen-3-yl acetate destabilizes NF-κB's binding to DNA, decreasing its ability to decrease p53 expression and moving towards apoptosis [23]. Oleanen-3-yl acetate's inhibition of STAT3 and NF-κB disrupts key pro-survival pathways in cancer, potentially leading to reduced tumor growth, enhanced apoptosis, and lowered resistance to treatment. This dual inhibition strategy highlights its promise as a therapeutic candidate for cancers driven by aberrant STAT3 and NF-κB signaling. Thus, these findings support the interaction of oleanen with different signaling molecules, supporting its activity in tumor-based inflammation. This multifaceted approach is supported by molecular docking and dynamics data, which illustrate the efficacy of Hemidesmus in modulating these critical signaling pathways in cancer.

CONCLUSION

This study details the ability of oleanen-3-yl acetate from Hemidesmus indicus to modulate different signaling pathways in STAT-3-mediated tumor inflammation. Simulation data revealed that oleanen exerts binding solid affinity, particularly with receptors such as STAT3, NF-κB p105, and p53, with binding energies especially less than -5 kcal/mol with STAT3, reporting to be -8.1 kcal/mol. This supports the current understanding of STAT3-NF-κB interaction, which decreases the transcription of genes that promote cell survival. The simulation data depicts the fluctuations in the internal energy of the bound protein-ligand complex caused by oleanen-3-yl acetate. RMSD and RMSF data indicate that interactions cause conformational changes, leading to apoptosis. This study demonstrates the potential of oleanen-3-yl acetate as a promising therapeutic agent by targeting critical signaling pathways like STAT3 and NF-κB involved in tumor inflammation. The strong binding affinity and stable interactions observed through molecular docking and dynamics simulations suggest its efficacy in disrupting cancer-related pathways. Given these results, oleanen-3-yl acetate shows significant promise for clinical applications as a dual inhibitor of STAT3 and NF-κB, paving the way for developing novel anti-cancer therapies. Further experimental validation and in vivo studies are warranted to confirm its therapeutic potential. The next steps in validating oleanen-3-yl acetate include conducting in-vitro studies to assess its cytotoxicity and inhibitory effects on cancer cell lines, followed by in-vivo studies to evaluate its pharmacokinetics, safety, and therapeutic efficacy in animal models. These experiments will help bridge the gap between simulation results and clinical application. This research supports that oleanen-3-yl acetate has an intense activity in tumor inflammation mediated through STAT-3 signaling, with further questions in future experimental validation.

FINANCIAL ASSISTANCE

NIL

CONFLICT OF INTEREST

The authors declare no conflict of interest.

AUTHOR CONTRIBUTION

J Renukadevi contributed to drafting the manuscript's content and articulating the research findings and discussions, contributing to technical coherence and quality. V S Karthikha J. Sam Helinto, D. Prena, Arockiya Rabin. A contributed equally to formatting and editing the manuscript**.**

REFERENCES

[1] Asma ST, Acaroz U, Imre K, Morar A, Shah SRA, Hussain SZ, Arslan-Acaroz D, Demirbas H, Hajrulai-Musliu Z, Istanbullugil

FR, Soleimanzadeh A, Morozov D, Zhu K, Herman V, Ayad A, Athanassiou C, Ince S. Natural products/bioactive compounds as a source of anticancer drugs. *Cancers (Basel)*, **14**, 6203 (2022) https://doi.org/10.3390/cancers.14246203.

[2] Varadarajan PS, Roy A, Jagadeswaran D. Anticancer property of Digera muricata leaf extract: An in vitro study. *Cureus*, (2023) https://doi.org/10.7759/cureus49276.

[3] Chang Y, Hawkins BA, Du JJ, Groundwater PW, Hibbs DE, Lai F. A guide to in silico drug design. *Pharmaceutics*, **15**, 49 (2022) https://doi.org/10.3390/pharmaceutics15010049.

[4] Singh N, Vayer P, Tanwar S, Poyet J-L, Tsaioun K, Villoutreix BO. Drug discovery and development: introduction to the general public and patient groups. *Front. Drug Discov. (Lausanne)*, **3**, (2023) https://doi.org/10.3389/fddsv.2023.1201419.

[5] Patel K, Patel J, Patel M, Rajput G, Patel H. Introduction to hyphenated techniques and their applications in pharmacy. *Pharm. Methods*, **1**, 2 (2010). https://doi.org/10.4103/2229-4708.72222.

[6] Hughes JP, Rees S, Kalindjian SB, Philpott KL. Principles of early drug discovery. *Br. J. Pharmacol.*, **162**, 1239–49 (2011). https://doi.org/10.1111/j.1476-5381.2010.01127.x

[7] Agu PC, Afiukwa CA, Orji OU, Ezeh EM, Ofoke IH, Ogbu CO, Ugwuja EI, Aja PM. Molecular docking as a tool for the discovery of molecular targets of nutraceuticals in diseases management. *Sci. Rep.*, **13**, (2023). https://doi.org/10.1038/s41598-023-40150-2.

[8] Salo-Ahen OMH, Alanko I, Bhadane R, Bonvin AMJJ, Honorato RV, Hossain S, Juffer AH, Kabedev A, Lahtela-Kakkonen M, Larsen AS, Lescrinier E, Marimuthu P, Mirza MU, Mustafa G, Nunes-Alves A, Pantsar T, Saadabadi A, Singaravelu K, Vanmeert M. Molecular dynamics simulations in drug discovery and pharmaceutical development. *Processes (Basel)*, **9**, 71 (2020) https://doi.org/10.3390/pr9010071.

[9] Turrini E, Catanzaro E, Muraro MG, Governa V, Trella E, Mele V, Calcabrini C, Morroni F, Sita G, Hrelia P, Tacchini M, Fimognari C. *Hemidesmus indicus* induces immunogenic death in human colorectal cancer cells. *Oncotarget*, **9**, 24443–56 (2018). https://doi.org/10.18632/oncotarget.25325.

[10] Aldughaylibi FS, Raza MA, Naeem S, Rafi H, Alam MW, Souayeh B, Farhan M, Aamir M, Zaidi N, Mir TA. Extraction of bioactive compounds for antioxidant, antimicrobial, and antidiabetic applications. *Molecules*, **27**, 5935 (2022). https://doi.org/10.3390/molecules27185935.

[11] Devi JR, Devi GN, Bavanilatha M, Gayathri G, Kowsalyaleela K, Anusha S, Durga M, Ramani R, Sabitha K. Pharmacophore based QSAR modelling of natural leads in antimicrobial drug design. *Current Chinese Chemistry*, **1**, 80–4 (2021). https://doi.org/10.2174/2666001601666200206102612.

[12] Meng X-Y, Zhang H-X, Mezei M, Cui M. Molecular docking: A powerful approach for structure-based drug discovery. *Curr. Comput. Aided Drug Des.*, **7**, 146–57 (2011) https://doi.org/10.2174/157340911795677602.

[13] Vidhya Rekha U, Rajagopal P, Varadhachariyar R, Harie Priya P, Shazia Fathima JH, Govindan R, Palanisamy C, Aswini Brindha KB, Veeraraghavan VP, Jayaraman S. Molecular docking analysis of bioactive compounds from Cissampelos pareira with PPAR gamma. *Bioinformation*, **18**, 265–8 (2022) https://doi.org/10.6026/97320630018265.

[14] Dilipkumar, Karthik, Gowramma, Magesh, Kaviarasan. Synthesis, characterization, docking studies, and in-vitro cytotoxic activity of some novel 2, 3 disubstituted naphthalene 1,4 Dione derivatives. *Curr. Bioact. Compd.*, **20**, (2024) https://doi.org/10.2174/0115734072298465240403084903

[15] Nautiyal M. Molecular docking analysis of Indole based diaza-sulphonamides with JAK-3 protein. *Bioinformation*, **19**, 74–8 (2023) https://doi.org/10.6026/97320630019074.

[16] Ramasubburayan R, Amperayani KR, Varadhi G, Dhanraj G, Athista M, Mahapatra S, Prakash S. Unraveling bioactive metabolites of mangroves as putative inhibitors of SARS-CoV-2 Mpro and RBD proteins: molecular dynamics and ADMET analysis. *J. Biomol. Struct. Dyn.*, 1–10 (2023) https://doi.org/10.1080/07391102.2023.2275185.

[17] Mao Q, Feng M, Jiang XZ, Ren Y, Luo KH, van Duin ACT. Classical and reactive molecular dynamics: Principles and applications in combustion and energy systems. *Prog. Energy Combust. Sci.*, **97**, 101084 (2023). https://doi.org/10.1016/j.pecs.2023.101084.

[18] Satish S. Molecular docking analysis of protein filamin-A with thioazo compounds. *Bioinformation*, **19**, 99–104 (2023). https://doi.org/10.6026/97320630019099.

[19] Das P, Mattaparthi VSK. Computational investigation on the p53–MDM2 interaction using the potential of mean force study. *ACS Omega*, **5**, 8449–62 (2020). https://doi.org/10.1021/acsomega.9b03372.

[20] Lobanov MI, Bogatyreva NS, Galzitskaia OV. Radius of gyration is indicator of compactness of protein structure. *Mol. Biol. (Mosk.)*, **42**, 701–6 (2008). https://doi.org/10.1134/S0026893308040195.

[21] Krajka-Kuźniak V, Belka M, Papierska K. Targeting STAT3 and NF-κB signaling pathways in cancer prevention and treatment: The role of chalcones. *Cancers (Basel)*, **16**, 1092 (2024) https://doi.org/10.3390/cancers.16061092.

[22] Pandey B, Grover A, Sharma P. Molecular dynamics simulations revealed structural differences among WRKY domain-DNA interaction in barley (Hordeum vulgare). *BMC Genomics*, **19**, (2018) https://doi.org/10.1186/s12864-018-4506-3.

[23] Carrà G, Lingua MF, Maffeo B, Taulli R, Morotti A. P53 vs NF-κB: the role of nuclear factor-kappa B in the regulation of p53 activity and vice versa. *Cell. Mol. Life Sci.*, **77**, 4449–58 (2020) https://doi.org/10.1007/s00018-020-03524-9.